AJNR

Comparison of MR and CT Myelography in Imaging the Cervical and Thoracic Spine

Michael G. Karnaze, Mokhtar H. Gado, Klaus J. Sartor and Fred J. Hodges III

Comparison of MR and CT Myelography in Imaging the Cervical and Thoracic Spine

Michael G. Karnaze[1]
Mokhtar H. Gado
Klaus J. Sartor
Fred J. Hodges III

MR imaging and CT myelography were compared in a retrospective study of 38 patients with suspected lesions of the cervical and thoracic spinal canal and cord. Twenty-eight abnormal cases were found, including spondylosis (9), tumors (8), intramedullary cavities (3), arachnoiditis (3), disk-space-centered infection or osteomyelitis (2), nonneoplastic cord swelling (2), and CSF-borne metastasis (1).

MR was equal or superior to CT myelography in depicting cases of cord enlargement, cord compression, and cord atrophy, providing better tissue characterization, no shoulder artifact, and no limitation caused by CSF block. CT myelography was superior to MR in depicting cases of spondylosis and arachnoiditis. It showed superior spatial resolution, which was most pronounced when comparing axial images and hence particularly superior in detecting the lateral extent of disk herniation. Use of surface coils and thin imaging sections is essential for accurate and complete MR evaluation of the cervical and thoracic spine.

CT has been accepted as an effective imaging technique for evaluating the spine. Its use, however, is limited in the cervical and thoracic spine because of the lack of epidural fat in this region. CT myelography performed after intrathecal introduction of water-soluble contrast material improves the contrast sensitivity of CT, but it is invasive and has known side effects [1–7].

Numerous reports have described the potential of MR as a valuable method of imaging the spine, and have compared MR with CT and CT myelography [8–15]. To help determine the role of MR in the evaluation of the cervical and thoracic spine, a comparative study of MR and high-resolution CT myelography was performed.

Materials and Methods

We retrospectively reviewed 38 patients with suspected lesions of the cervical or thoracic spine who underwent both MR and CT myelography. No effort was made to conceal the diagnoses from the reviewers. The patients ranged in age from 1–75 years; 18 were males and 20 were females. In 10 cases no abnormality was found by either imaging technique. The 28 abnormal findings included nine cases of spondylosis, eight neoplasms, three cases of arachnoiditis, three intramedullary cavities, two cases of disk-space infection, two cases of nonneoplastic cord swelling, and one case of CSF-borne metastases. Seventeen cases involved the cervical and 11 involved the thoracic spine.

Surgical or pathologic proof was available in 16 abnormal cases, and clinical and radiographic evidence was available in the remaining 12.

MR was performed with a Siemens Magnetom 0.5-T (initially operating at 0.35 T) or 1.5-T unit. Spin echo (SE) sequences were used yielding three images of the same anatomic level: a T1-weighted image (TR 300 or 500 msec, TE 30 msec), a spin-density-weighted image (TR 1500 or 1800 msec, TE 30 msec), and a T2-weighted image (TR 1500 or 1800 msec, TE 120 msec). A body coil was used in seven cases, a head coil was used in nine cases, and a surface coil was used in 12 cases. Slice thickness was 5 mm for all surface-coil images except one case, in which a 10-mm thickness was used. Ten-millimeter sections were used

for all head- and body-coil images except one case, in which the head coil and 5-mm sections were used. Sagittal images were obtained in all cases, axial images in 18, and coronal images in five. Images were processed on a 256 × 256 matrix corresponding to 1.2-mm² pixel size in all examinations.

CT images were obtained after myelography with water-soluble contrast material on a third-generation scanner*, using 2.0-mm axial scans. Delayed CT scanning 8–24 hr after initial examination was performed in four cases.

In the 38 cases, 43 final *radiologic* diagnoses were made and these were divided into six categories: normal (10), cord swelling (eight), cord atrophy (seven), cord compression (10), extradural lesions without cord compression (five), and arachnoiditis (three). Five of the 28 abnormal cases were included in two different radiologic categories, yielding 33 total abnormal final diagnoses. CT scans and MR images were compared to evaluate the ability of each imaging technique to detect the abnormality and to determine its cause. Reasons for failure or superiority of MR compared with CT myelography were noted.

Results

In the 10 normal cases, MR and CT myelography were equivalent in depicting the normal cord and surrounding CSF space. In the remaining 33 radiologic diagnoses, MR was superior to CT myelography in nine instances, equivalent in 13, and inferior in 11. Results are summarized in Tables 1–4. The remaining five radiologic diagnoses will be discussed separately.

Cord Enlargement

In all eight cases, cord enlargement (Table 1) was detected equally well by MR and CT myelography. However, MR was superior to CT myelography in determining the cause of the abnormality in three cases. In one case of hematomyelia (Fig. 1), CT myelography showed nonspecific cord enlargement while MR showed increased signal of the lesion on the T1- and T2-weighted images. The chemical-shift-imaging technique [16] was employed and showed this to be due to hemorrhage, not to fat. MR was superior in another case of an intramedullary cord cyst at the level of T2, in which MR showed the cavity, which was not seen with delayed CT myelography because of shoulder artifacts. The third case in which MR was superior was one of ependymoma of the cervical cord. CT myelography showed low-density enlargement of the cord. MR showed both the soft-tissue and fluid components of the lesion, confirming that it was a tumor and not a congenital hydromyelia. In no case of cord enlargement was CT myelography superior to MR.

Cord Atrophy

In seven cases of cord atrophy (Table 2) MR was equal to CT myelography in detecting the abnormally small cord in three cases and inferior to CT myelography in four cases. In one of these four cases, MR using surface coil and 5-mm sections showed the atrophic cord but failed to detect a 2-

*Siemens Somatom 2, DR3 or DRH.

TABLE 1: Cord Swelling

Case No.	Age	Gender	Diagnosis	MR Coil	MR (Compared with CT Myelography)
1	75	F	Ependymoma[a]	Surface	Superior
2	52	M	Thoracic cord cyst	Surface	Superior
3	41	M	Cord hemorrhage[a]	Head	Superior
4	16	M	Radiation myelitis	Head	Equivalent
5	41	F	Intradural CSF metastasis	Head	Equivalent
6	35	F	Myelitis[a]	Head	Equivalent
7	2	F	Glioma[a]	Body	Equivalent
8	8	F	Intramedullary tumor	Body	Equivalent

[a] Histologically confirmed.

TABLE 2: Cord Atrophy

Case No.	Age	Gender	Etiology	MR Coil	MR (Compared with CT Myelography)
9	26	M	Cord cavity	Surface	Inferior
10	40	F	Surgery	Surface	Equivalent
11	62	F	Surgery	Surface	Equivalent
12	42	M	Trauma	Head	Equivalent
13	34	F	Unknown	Body	Inferior
14	53	M	Cavity[a]	Body	Inferior
15	38	F	Unknown	Body	Inferior

[a] Histologically confirmed.

TABLE 3: Cord Compression

Case No.	Age	Gender	Diagnosis	MR Coil	MR (Compared with CT Myelography)
16	71	F	Meningioma	Surface	Superior
17	48	M	Herniated cervical disk[a]	Surface	Superior
18	33	M	Herniated cervical disk[a]	Surface	Inferior
19	51	F	Herniated thoracic disk	Surface	Superior
20	39	M	Meningioma[a]	Surface	Superior
21	73	M	Extruded disk fragment	Head	Superior
22	66	M	Cervical subluxation[a]	Head	Inferior
23	41	F	Intradural metastasis	Head	Equivalent
24	44	M	Vertebral osteomyelitis[a]	Body	Equivalent
25	51	M	Schwannoma[a]	Body	Inferior

[a] Histologically confirmed.

TABLE 4: Extradural Lesions Without Cord Compression

Case No.	Age	Gender	Diagnosis	MR Coil	MR (Compared with CT Myelography)
26	66	F	Disk space infection[a]	Surface	Superior
27	39	M	Cervical disk herniation[a]	Surface	Inferior
28	47	M	Cervical bony bars[a]	Head	Inferior
29	52	F	Cervical disk bulge	Head	Equivalent
30	50	M	Cervical bony bars	Body	Equivalent

[a] Histologically confirmed.

Fig. 1.—Hematomyelia.

A, CT myelogram shows focal nonspecific cord enlargement (*arrow*).

B, Proton-density-weighted MR image shows high signal from hemorrhage. High signal was also present on T1-and T2-weighted images (not shown).
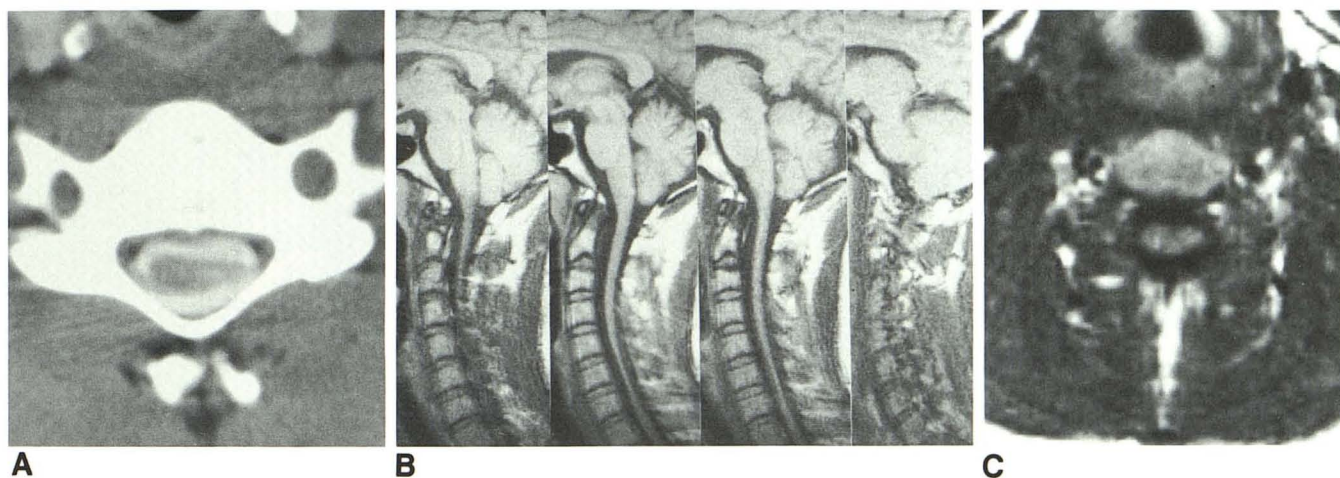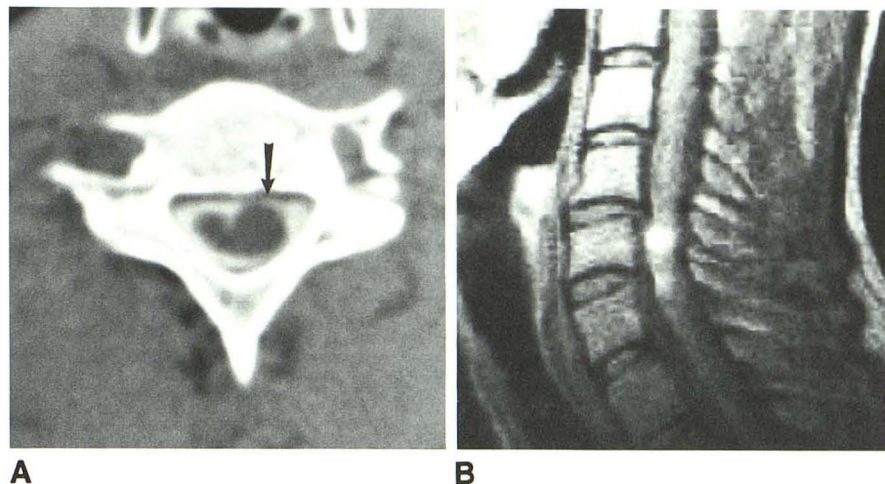

A   B

A   B   C

Fig. 2.—Cord atrophy with small cavity.

A, CT myelogram shows atrophic cord and 2-mm contrast-filled cavity in left side of cord.

B, Series of contiguous T1-weighted MR images shows atrophy but fails to demonstrate cavity.

C, Axial T1-weighted MR image shows poor spatial resolution and is much less informative than CT myelogram (see *A*).

mm associated cavity, which was 3 cm in length and was seen on delayed CT scans (Fig. 2). In the other three cases in which MR was inferior, slice thickness was 10 mm and body coil was used, resulting in low spatial resolution. These three cases included a case of atrophy with associated cord arteriovenous malformation, a posttraumatic cavity, and atrophy associated with arachnoiditis. In no case of cord atrophy was MR superior to CT myelography.

Cord Compression

In 10 cases of cord compression (Table 3) MR was superior to CT myelography in five cases, equivalent in two cases, and inferior in three cases. In two of the three cases in which MR was inferior (a cervical intradural schwannoma and a cervical disk herniation), slice thickness was 10 mm and surface coil was not used. In the third case, a herniated cervical disk, CT myelography showed the lateral extent of disk herniation

better than MR did, and although surface-coil imaging and 5-mm sections were used, neither axial nor interdigitated images were obtained. Of the five cases in which MR was superior, two cases (a cervical disk herniation and a case of a presumed extruded disk fragment) showed serious degradation of the CT myelography images by shoulder artifacts. In a third case (of presumed thoracic disk herniation), MR allowed better differentiation of the compressed cord, narrowed CSF space, and thoracic disk than CT myelography did (Fig. 3). In the remaining two cases (meningiomas of the thoracic spine), CT myelography showed only the inferior margin of the lesion because of CSF block. No attempts were made to position water-soluble contrast material above the lesion. MR in these two cases showed the upper border and true size of the lesion and its interface with the cord (Fig. 4). In addition, both these lesions demonstrated a low signal intensity on the T2-weighted image, a feature previously reported in intracranial meningiomas [17].
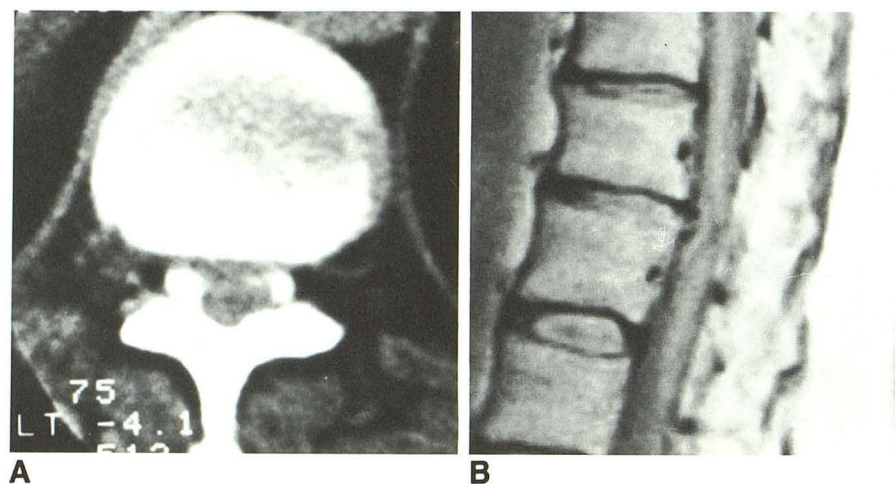
Fig. 3.—Presumed thoracic disk herniation.
A, CT myelogram at level of T11–T12 shows soft-tissue density anterior to cord. Differentiating cord from disk is difficult.
B, Sagittal proton-density-weighted MR image shows cord displaced posteriorly at level of disk space. Cord is well differentiated from disk.
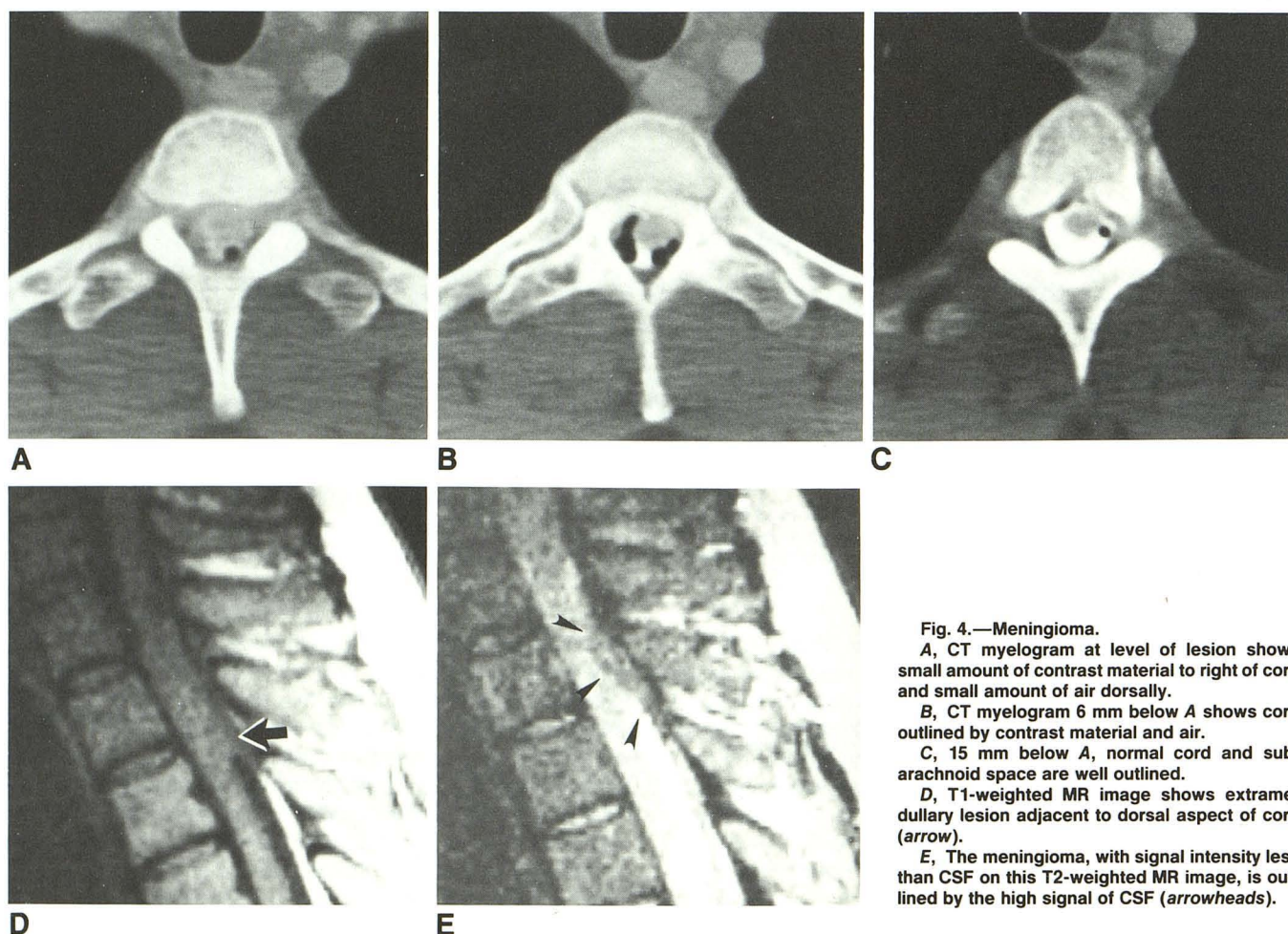

Fig. 4.—Meningioma.
A, CT myelogram at level of lesion shows small amount of contrast material to right of cord and small amount of air dorsally.
B, CT myelogram 6 mm below A shows cord outlined by contrast material and air.
C, 15 mm below A, normal cord and subarachnoid space are well outlined.
D, T1-weighted MR image shows extramedullary lesion adjacent to dorsal aspect of cord (arrow).
E, The meningioma, with signal intensity less than CSF on this T2-weighted MR image, is outlined by the high signal of CSF (arrowheads).

Extradural Lesions Without Cord Compression

In five cases of extradural lesions without cord compression (Table 4), MR was superior to CT myelography in one case, equivalent in two cases, and inferior in two cases. MR was superior in a case of disk-space-centered infection by showing decreased signal in the disk space and adjacent vertebral bodies on the T1-weighted images secondary to infection (Fig. 5). Both MR and CT myelography showed the paravertebral mass and the mild extradural encroachment on the anterior aspect of the subarachnoid and epidural spaces. The changes in the vertebral body were not convincing on CT

Fig. 5.—Disk-space-centered infection.

A, CT myelogram shows paravertebral mass and extradural soft-tissue density ventral to cord causing narrowing of subarachnoid space (arrow). Vertebral body shows mild focal loss of bone density ventrally.

B, Sagittal T1-weighted MR image demonstrates abnormally decreased signal from two adjacent vertebral bodies and some loss of signal from disk space. Extradural extension ventral to cord is also seen (arrow).

A   B
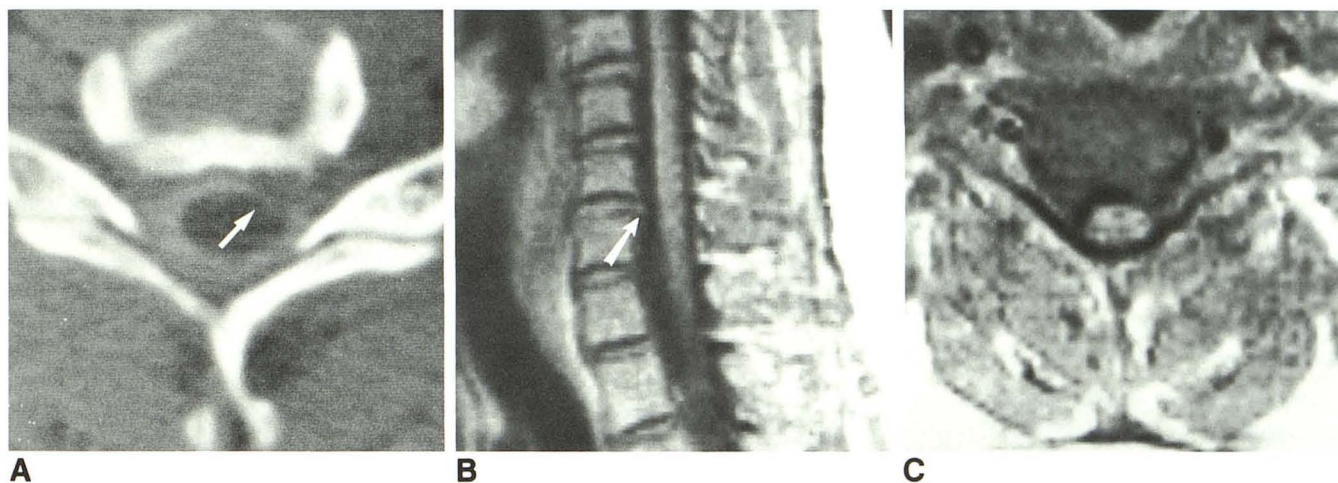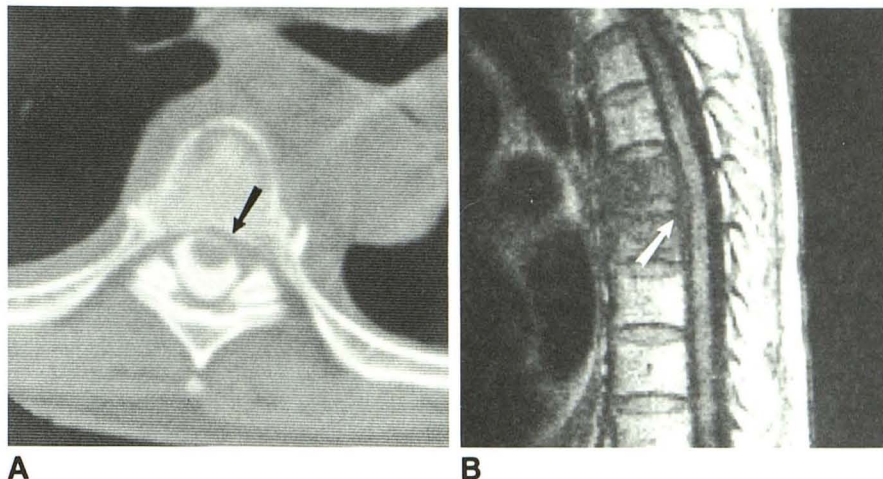

A   B   C

Fig. 6.—Cervical disk herniation.
A, Axial CT myelogram shows soft-tissue density anterior and lateral to cord with narrowing of subarachnoid space (arrow).
B, Sagittal T1-weighted MR image shows bulging of C6–C7 disk (arrow).
C, Axial T1-weighted MR image fails to show lateral extent of disk as well as CT did.

myelography. On MR, however, the vertebral body changes were clearly demonstrated and the nature of the process was defined as bone-centered. The clinical management was planned accordingly. In one case of osteophytes indenting the subarachnoid space and the intervertebral foramina in the cervical spine, MR was inferior to CT myelography. The case was imaged with a head coil and 10-mm sections. However, in another case in which a surface coil and 5-mm sections were employed, CT myelography was superior to MR because superior spatial resolution allowed CT to show the lateral extent of a cervical disk herniation better than MR did (Fig. 6).

Arachnoiditis

In three cases of arachnoiditis, MR was equivalent to CT myelography in one case and inferior in two cases. In one of

the cases in which MR was inferior, MR did provide complementary information by showing no lesion at a site of CSF block on CT myelography. Although MR alone would have missed the diagnosis, lack of abnormal signal from the site of the CSF block indicated arachnoid adhesions and not a mass as the cause of the block on CT myelography. In this case and in one other case, MR did not show arachnoid adhesions or multiple loculated pockets of CSF that were evident on CT myelography.

Coil Selection

The importance of surface-coil imaging in evaluating the cervical and thoracic spine is demonstrated in Table 5. Regardless of the diagnostic category, a surface coil was used in 14 cases, of which MR was superior to CT myelography in seven, equivalent in three, and inferior in four. On the other

TABLE 5: Value of Surface-Coil Imaging

	No. of Cases	Comparison of MR and CT Myelography		
		MR Superior	Equal	MR Inferior
Surface coil	14	7	3	4
Nonsurface coil	19	2	10	7
Total	33	9	13	11

TABLE 6: Advantages of MR over CT Myelography in 11 Cases

Tissue specificity (n = 6)
  Hematomyelia
  Cervical ependymoma
  Thoracic disk herniation
  Disk-space-centered infection
  Meningioma (n = 2)
Lack of shoulder artifact (n = 3)
  Cervical disk herniation
  Thoracic cord cavity
  Presumed extruded disk fragment
No limitation from CSF block (n = 2)
  Meningioma

hand, in the 19 cases in which a surface coil was not used, MR was superior in only two cases, equivalent in 10, and inferior in seven.

Discussion

MR compares favorably with CT myelography in cases of cord swelling and those of cord atrophy and compression if a surface coil and thin sections are used. Advantages of MR include tissue characterization, lack of shoulder artifact, and complete delineation of the lesion in spite of CSF block (Table 6). The contribution of tissue characterization was significant in six of our 33 abnormal diagnoses. Cord hemorrhage (Fig. 1) was characterized by a relative signal increase on both T1- and T2-weighted images. Although fat-containing tumors could have a similar appearance on T1-weighted images, a chemical-shift technique [16] can be used to distinguish the two conditions. Disk-space-centered infection (Fig. 5) was characterized by low signal from the disk space and adjacent vertebral bodies on T1-weighted images, an appearance previously described [18]. In the case of the presumed thoracic disk herniation (Fig. 3), MR differentiated cord, vertebral body, and disk. Because of the lack of difference in density between the cord and disk and the lack of contrast material anteriorly and posteriorly at the level of the lesion, CT myelography did not identify clearly the cord-disk interface. The diagnosis of disk herniation was therefore not made before MR was performed. MR also detected the solid component of a cervical ependymoma by a signal intensity pattern different from parenchyma and CSF. CT myelography could not differentiate a cystic tumor from a syrinx. In two additional cases of thoracic meningioma, the relatively low signal of the lesion on the T2-weighted image suggested the diagnosis, as these signal characteristics have been noted in intracranial meningiomas [17].

Degradation of CT images is common in the lower cervical region and at the cervical thoracic junction. This is caused by the sudden increase in X-ray attenuation at the level of the shoulders. This takes the form of dense, dark streaks across the images [19]. The degradation often results in total loss of the diagnostic image at that level. No such degradation is known in MR, and signal intensity is not attenuated by surrounding tissues. Imaging by MR is far superior than by CT myelography in this region, as was shown in three cases in our series.

Another limitation of CT myelography is seen in cases in which a space-occupying lesion causes block to CSF flow. The contrast material is stopped by the lesion and outlines the lower border of the lesion only. To determine the full extent of the lesion and outline its upper border, contrast material may be introduced by high cervical puncture. Alternatively, the contrast material that has been stopped below the site of the block may be forced to cross the block using a "squeeze" technique [20]. Neither of these techniques was used in our series. High cervical puncture adds to the invasiveness of the procedure. The squeeze technique is reportedly without risk; however, its potential added risk cannot be evaluated until a large series is reported. MR provides complete imaging of the lesion noninvasively.

Although MR was equal or superior to CT myelography in cord enlargement regardless of the coil used, cases of cord compression and atrophy demonstrate the need for surface coils in examining the spine (see Tables 2 and 3). Eight cases of cord compression and atrophy were examined with surface coils. MR was superior to CT myelography in four and equivalent in two. On the other hand, MR was inferior in five and equivalent in three of nine cases with the same diagnoses examined without surface coils.

MR failed in 11 of our cases. However, in eight of these cases the MR technique was suboptimal. The slice thickness was 10 mm and the surface coil was not used early in our experience with the method. There remain three cases in which the proper technique was used. Analysis of these three cases attributed the failure of MR to low spatial resolution, particularly in axial images. For this reason, CT myelography showed to a better advantage a 2-mm cervical cord cavity (Fig. 2). The added high-contrast discrimination caused by entry of contrast material into the cavity enhanced the spatial resolution. For the same reason, the lateral extent of herniated cervical disk was not demonstrated by MR (Fig. 6), and small CSF pockets outlined by arachnoid adhesions were also missed by MR but well shown by CT myelography. However, the absence of abnormal findings on MR in cases of arachnoiditis is not without diagnostic value. Indeed, deformity of the contrast column on myelography and CT myelography may mimic the presence of intradural or extradural lesions. The possibility of such lesions can easily be excluded by the normal appearance on MR images, as shown in one of three cases of arachnoiditis in our series.

The poor quality of axial images as compared with sagittal images on MR limits the usefulness of this technique in

evaluating lateral lesions. Furthermore, sagittal images are difficult to interpret in cases of scoliosis.

Our results suggest that MR can serve as the primary imaging tool in evaluation of the cervical and thoracic spine. If a surface coil is used, MR is equivalent or superior to CT myelography in cases of cord swelling, cord atrophy, and cord compression. CT myelography, however, appears equal or superior to MR in cases of spondylosis and arachnoiditis. It will likely remain so until improved axial images can be generated with MR. Although not addressed in this study, plain CT of the cervical and thoracic spine could perhaps adequately complement MR in showing bony detail and intervertebral foramina, thus significantly decreasing the need for myelography.

Conclusions

MR was equal or superior to CT myelography in our study in categories of cord swelling, cord atrophy, and cord compression. It provided additional information in six of 33 cases because of improved tissue characterization, in three cases because of lack of shoulder artifact, and in two cases with CSF block. CT myelography offers superior spatial resolution, which was important in four cases. CT was equivalent or superior to MR in cases of spondylosis and arachnoiditis. Surface-coil imaging and thin sections are essential if MR is to be used to evaluate the cervical and thoracic spine.

REFERENCES

1. Greitz T, Hindmarsh T. Computer assisted tomography of intracranial CSF circulation using water-soluble contrast medium. *Acta Radiol [Diagn] (Stockh)* **1974**;15:497–507
2. Di Chiro G, Schellinger D. Computed tomography of spinal cord after lumbar intrathecal introduction of metrizamide (computer assisted myelography). *Radiology* **1976**;120:101–104
3. Aubin ML, Vignaud J, Jardin C, Bar D. Computed tomography in 75 clinical cases of syringomyelia. *AJNR* **1981**;2:199–204
4. Dublin AB, McGahan JP, Reid MH. The value of computed tomographic metrizamide myelography in the neuroradiological evaluation of the spine. *Radiology* **1983**;146:79–86
5. Tadmor R, Cacayorin, Kieffer SA. Advantages of supplementary CT in myelography of intraspinal masses. *AJNR* **1983**;4:618–621
6. Landman JA, Hoffman JC Jr, Braun IF, Barrow DL. Value of computed tomographic myelography in the recognition of cervical herniated disk. *AJNR* **1984**;5:391–394
7. Sobel DF, Barkovich AJ, Munderloh SH. Metrizamide myelography and postmyelographic computed tomography: comparative adequacy in the cervical spine. *AJNR* **1984**;5:385–390
8. Bradley WG Jr, Waluch V, Yadley RA, Wycoff RR. Comparison of CT and MR in 400 patients with suspected disease of the brain and cervical spinal cord. *Radiology* **1984**;152:695–702
9. Han JS, Kaufman B, El Yousef JJ, et al. NMR imaging of the spine. *AJNR* **1983**;141:1137–1145
10. Modic MT, Weinstein MA, Pavlicek W, Boumphrey F, Starnes D, Douchesneau PM. Magnetic resonance imaging of the cervical spine: technical and clinical observations. *AJR* **1983**;141:1129–1136, *AJNR* **1984**;5:15–22
11. Norman D, Mills CM, Brant-Zawadzki M, Yeates A, Crooks LE, Kaufman L. Magnetic resonance imaging of the spinal cord and canal: potentials and limitations. *AJR* **1983**;141:1147–1152, *AJNR* **1984**; 5:9–14
12. Hyman RA, Edwards JH, Vacirca JJ, Stein HL. 0.6 T MR imaging of the cervical spine: multislice and multiecho techniques. *AJNR* **1985**;6:229–236
13. Pojunas K, Willliams AL, Daniels DL, Haughton VM. Syringomyelia and hydromyelia: magnetic resonance evaluation. *Radiology* **1984**;153:679–683
14. Lee BCP, Zimmerman RD, Manning JJ, Deck MDF. MR imaging of syringomyelia and hydromyelia. *AJNR* **1985**;6:221–228
15. Modic MT, Pavlicek W, Weinstein MA, et al. Magnetic resonance imaging of intervertebral disk disease. *Radiology* **1984**;152:103–111
16. Dixon WT. Simple proton spectroscopic imaging. *Radiology* **1984**;153:189–194
17. Zimmerman RD, Fleming CA, Saint-Louis LA, Lee BCP, Manning JJ, Deck MDF. Magnetic resonance imaging of meningiomas. *AJNR* **1985**;6:149–157
18. Modic MT, Feiglin DH, Piraino DW, et al. Vertebral osteomyelitis: assessment using MR. *Radiology* **1985**;157:157–166
19. Brooks RA, Di Chiro G. Beam hardening in X-ray reconstructive tomography. *Phys Med Biol* **1976**;21:390–398
20. Kelly WM, Badami P, Dillon W. Epidural block: myelographic evaluation with a single puncture technique using metrizamide. *Radiology* **1984**; 151:417–419